



**CHAPTER 4**  
**EXPERIMENTAL GALANTAMINE**  
**HYDROBROMIDE LOADED**  
**NANOPARTICLES**



#### **4.1 Introduction:**

Acetylcholine esterase inhibitors are the most successful class of therapeutic agents to decrease the progression of Alzheimer's disease. Out of that, Galantamine (GAL) is one such drug. It is approved by the USA FDA and the European Medicines Agency for the symptomatic treatment of Alzheimer's disease due to its ability to moderate acetylcholinesterase inhibition in the CNS. Gal is commercially available as tablets and oral suspension. However, when administered via the oral route, it leads to severe nausea and vomiting because of its motor and evacuative function on the intestinal tissues (V De Caro, G Giandalia, MG Siragua, G Campsisi, & Giannola, 2009). Additionally, recent reports have shown that Galantamine also has anti amyloid activity (Matharu et al., 2009). But to fully exploit its potential, it has to be delivered properly and that necessitates surpassing the Blood Brain Barrier (BBB).

Nanoparticles have been highly exploited for controlled and site – specific delivery of drugs. The site specific delivery of drugs by them has shown promising results for the treatment of various diseases including cancer, human immunodeficiency virus infection (Friese et al., 2000; Mitra et al., 2001). As compared with the bulk material, the formulated nanoparticles have a high surface /volume ratio, due to which its surface area increases leading to increase in drug loading, improved circulation in the body and thereby result in a reduction in the dose as well as the frequency of administration of the drug with a consequent increase in the patient compliance (Wilson et al., 2010). Due to the aforementioned properties, nanoparticles are also faring well in delivering drugs to brain (Peracchia et al., 1999).

Biodegradable polymers are always preferred over non biodegradable once for formulating nanoparticles. Proteins like albumin and gelatin are also used for formulating nanoparticles. Bovine serum albumin is a very versatile polymer, for drug delivery because of its medical importance, abundance, low cost, ease of purification, unusual ligand-binding properties and its wide acceptance in the pharmaceutical industry (Elzoghby, Samy, & Elgindy, 2012).

Optimization of any (Yu, 2008) process for pharmaceutical formulation begins with finding out and evaluating independent variables that affect formulation response, determine them and establish their best response values. However, considering the cost of the drugs and polymers, it is desirable to optimize the formulation development with minimum batches and maximum desired characteristics. Optimization by changing one-variable at-a-time is a complex method to evaluate the effects of different variables on an experimental outcome. This approach assesses one variable at a time instead of all simultaneously. The method is time-consuming, expensive and often leads to misinterpretation of results when interactions between different components are present. While developing formulations, various formulations as well as process variables related to effectiveness, safety and usefulness should be simultaneously optimized.

Quality by design (QBD) is based on the improvement of the quality of formulation at designing level. (Yu, 2008). This practice encourages building in quality rather checking its quality at the end of product development.

Studies based on factorial designs allow all the factors to be varied simultaneously, thus enabling evaluation of the effects of each variable at each level and showing interrelationship among them. The number of experiments required for these studies is dependent on the number of independent variables selected. Polynomial non-linear regression analysis are widely used for establishing approximate mathematical models in which the variables are screened by stepwise selection method according to statistical significance (AJ, 1984; Wagner & Shimshak, 2007) and final model is used to predict the relationship between different variables and their levels. But such predictions are often limited to low levels, resulting in poor estimation of optimum formulation (Levison, Takayama, Isowa, Okabe, & Nagai, 1994; Shirakura O et al., 1991). Therefore, it is important to understand the complexity of pharmaceutical formulations by using established statistical tools such as multiple regression analysis (MRA), full factorial design etc.

Quality by design is a more systematic approach to product development. It involves incorporation of prior knowledge, use of quality risk management, results of studies using design of experiments.

By following the principles of Quality by Design, the development of formulation should involve a minimum of the below mentioned elements:

- (1) Defining the quality target product profile as it relates to quality, safety and efficacy, considering e.g. the route of administration, dosage form, bioavailability, strength, and stability.
- (2) Identifying potential critical quality attributes of the drug product, so that those product characteristics having an impact on product quality can be studied and controlled.
- (3) Selecting an appropriate manufacturing process.
- (4) Defining a control strategy.
- (5) Identifying and assessing the risks.
- (6) Determining the functional relationships that link material attributes and process parameters to product Critical Quality Attributes.

#### Quality Target Product Profile:

The quality target product profile forms the basis of design for the development of the product. Considerations for the quality target product profile could include: intended use in clinical setting, route of administration, dosage form, delivery systems; Dosage strength(s); Container closure system; therapeutic moiety release or delivery and attributes affecting pharmacokinetic characteristics; drug product quality criteria appropriate for the intended marketed product.

#### Critical Quality Attributes:

A CQA is a physical, chemical, biological or microbiological property or characteristic that should be within an appropriate limit, range or distribution to ensure the desired product quality. CQAs are generally associated with the drug substance, excipients, intermediates and drug product.

**Risk Assessment:**

It is a science - based process used to understand which material attributes and process parameters potentially have an effect on product Critical Quality Attributes. It is typically performed early in the development of formulation and is repeated as more information and greater knowledge is obtained. It can be used as a tool to identify and rank parameters with potential to have an impact on product quality, based on prior knowledge and initial experimental data.

**Design space:**

The relationship between the process inputs (material attributes and process parameters) and the critical quality attributes can be described in the design space.

Defining the Design space requires selection of variables that can lead to an understanding of the linkage and effect of process parameters and material attributes on product CQAs, and also help identify the variables and their ranges within which consistent quality can be achieved. These process parameters and materials attributes can thus be selected for inclusion in the design space.

The design space can be constructed employing various approaches for experimental designing, like factorial design, response surface methodology etc.

Hence, the objective of this work was to develop nanoparticulate drug delivery system for Galantamine HBr with the aid of QbD for intranasal administration to improve its targeting to the real site that is the brain thereby reducing side effects. Such an endeavor is also expected to improve future market potential.

**4.2 Materials**

Galantamine hydrobromide was kindly gifted by SPARC, Vadodara, India; Bovine Serum Albumin (Fraction V, 98% purity) was purchased from Sigma Aldrich, India. Sodium carbonate was purchased from Qualigens, India. Distilled water was used for all experiments. Acetone, absolute alcohol, chloroform, isopropyl alcohol were procured from Spectra Chemicals, India.

### **4.3 Equipments and Instruments**

1. High speed magnetic stirrer (Remi, MS500, Remi equipment, India)
2. Digital pH meter (Lab India Ltd, India)
3. High speed centrifuge (Sigma 3K30, Germany)
4. Particle size Analyser (Zeta sizer Nano series, Malvern Instruments, UK)
5. UV – VIS spectrophotometer (UV 1800, Shimadzu, Japan)
6. Lyophilizer (Heto, Drywinner, Germany)
7. Differential Scanning Calorimeter (Shimadzu, Japan)
8. X- ray Diffractometer (Panalytical's Xpert Pro, Netherlands)
9. Transmission Electron Microscope (Tecnai 20, Philips, Holland)
10. Fourier Transform Infrared spectrophotometer (Bruker, Germany)
11. Atomic Force Microscopy ( Bruker Dimension Icon, USA)

### **4.4 Formulation of Galantamine HBr loaded nanoparticles by Desolvation-Thermal Gelation Method.**

#### *4.4.1 Optimization of Blank nanoparticles(Merodio, Arnedo, Renedo, & Irache, 2001)*

The formulation of nanoparticles from Bovine Serum Albumin can be done by various techniques like desolvation (coacervation), thermal gelation, nano spray drying etc. Out of all these methods, desolvation is a simpler technique that yields smaller particle size.

Prior to the formulation of drug loaded nanoparticles, blank nanoparticles were formulated and optimized for particle size. The procedure for the same is mentioned below.

Weighed quantity of Bovine Serum Albumin was dissolved in water. The pH of the solution was adjusted towards the alkaline side (pH = 8) using 0.1 M Na<sub>2</sub>CO<sub>3</sub> solution. To this solution, desolvating agent was added dropwise under magnetic stirring. After desolvation, the dispersion was heated to 75°C to evaporate the desolvating agent and also to cause the thermal gelation of Albumin.

The batches of nanoparticles were subjected to centrifugation (30 K, Sigma, Germany) at various RPM for sedimenting and collecting the nanoparticles.

The nanoparticles were optimized for following parameters on the basis of particle size:

(1) Choice of desolvating agent:

The desolvating agents chosen were acetone, absolute alcohol, chloroform, isopropyl alcohol. The particle size was determined.

(2) Rate of addition of desolvating agent:

The rate of addition of desolvating agent was varied on ml/min basis. The particle size was determined.

(3) Bovine Serum albumin content in the solution:

The Bovine serum albumin content was varied from 6.25 mg/mL to 25 mg/mL based on various literature reports. The particle size was determined.

(4) Centrifugation speed for collecting nanoparticles:

The speed of centrifuge was progressively increased to the point a pellet of nanoparticles was obtained along with a clear supernatant.

#### *4.4.2 Optimization of Galantamine hydrobromide loaded nanoparticles*

The Galantamine hydrobromide loaded nanoparticles were prepared by dissolving BSA (50 mg) in 4 ml of distilled water. The pH of this solution was adjusted between 8 – 9 with 0.1 M Na<sub>2</sub>CO<sub>3</sub>. Weighed amount of Galantamine hydrobromide (5 mg) was incubated with this Albumin solution for different duration of time (from 0.5 to 4 hour). This aqueous phase was desolvated with acetone by slowly adding it drop wise, slowly through a 1 ml syringe fitted with a 23 bore needle under magnetic stirring provided with heating plate (Remi Instruments, India). This system was subsequently heated to a temperature of 75°C for acetone evaporation and thermal gelation. The

nanoparticles obtained were separated by centrifugation at 35,000 RPM, at 4° C for 30 minute (Optima L-100XP, Beckmann, USA) which aided in separating the nanoparticles from free drug. The formed nanoparticles were then subjected to further characterization.

The Galantamine loaded Bovine Serum Albumin nanoparticles were optimized using the principles of Quality by Design, that is defining the Quality Target Product Profile, understanding and identifying the risks, risk assessment and finally experimental design to optimize the formulation and identify the design space.

#### 4.4.2.1 Risk Identification

Before the Galantamine hydrobromide nanoparticles were prepared, the critical qualities to be monitored were identified and termed as Critical Quality Attributes. These are the identification of attributes related to the formulation and the process parameters regarding the above mentioned manufacturing method. An Ishikawa diagram (Fish – bone diagram) was constructed to have a better understanding of the CQAs and the potential risks. On the basis of prior scientific knowledge, average particle size and encapsulation efficiency were considered as important CQAs of Galantamine hydrobromide nanoparticles as these parameters are likely to contribute substantially to the therapeutic efficacy (Vogt & Kord, 2011).

Failure mode and effect analysis (FMEA) method is another way of conducting risk analysis for a product to be developed. In this type of analysis, each variable (which has a potential to cause failure) was scored in terms of severity (S), detectability (D) and probability (P). From these the Risk Priority Number was calculated (Kan, Lu, Liu, Wang, & Zhao, 2014).

The factors with high RPN were subjected to further studies to ensure product safety and efficacy while those with lower RPN were eliminated from further studies.

The QTPP and CQA for Galantamine hydrobromide nanoparticles are shown in Table 4.1.

Table 4.1: Quality Target Product Profile and Critical Quality Attributes for Galantamine hydrobromide Nanoparticles. (FDA, 2012; ICH, 2009; Pallagi, Ambrus, Szabo-Revesz, & Csoka, 2015)

|                           | <b>Target</b>  | <b>Justification</b>   |
|---------------------------|--|--|
| <b>QTPP Elements</b>      |  |  |
| Target patient population | Adults   | Alzheimer’s disease affects adults   |
| Route of administration   | Nasal  | To surpass the gastric irritation, achieve brain targeting.  |
| Dosage form               | White to off white pharmaceutically elegant lyophilized cake that can be easily reconstituted. | Lyophilization required for long term stability of nanoparticles, elegant appearance needed for patient acceptability. Ease of reconstitution required for ensuring the delivery of dispersed nanoparticles to the dorsal part of nasal cavity |
| Dosage design             | Nasal spray  | For delivery to nasal cavity   |
| Pharmacokinetics          | Acceptable parameters to demonstrate therapeutic effect.                                       | Needed to understand the bioavailability after nasal administration.   |
| Stability                 | Stability in lyophilized condition   | Needed for quality and efficacy throughout the shelf life  |
| Container Closure System  | Container closure system qualified as suitable for   | Needed to achieve the target shelf-life and to ensure  |

|                                      |                                |  |
|--------------------------------------|--------------------------------|--|
|                                      | this drug product              | proper integrity of the product.   |
| Alternative method of administration | None                           | It is a suggested QTPP by the US FDA   |
| <b>CQA</b>                           |                                |  |
| Particle Size                        | Less than 200 nm               | Needed for efficient nose to brain targeting.                                      |
| Zeta Potential                       | In the range of -30 to + 30 mv | Provides physical stability to nanoparticles and prevents them from agglomerating. |
| Entrapment Efficiency                | Above 50%                      | High entrapment efficiency desirable to minimize drug loss during manufacturing    |
| Structure                            | Amorphous                      | Better dissolution and absorption <i>in vivo</i> .                                 |
| Cellular Toxicity                    | Non toxic                      | Desirable that carrier and nanoparticles should be non toxic                       |

#### 4.4.2.2 Risk Analysis by Plackett Burman design

Based on the outcomes of FMEA, further analysis of risk was studied using the Plackett Burman design (Rahman, Zidan, Habib, & Khan, 2010). A total of six factors were selected from FMEA studies. These factors were varied at two levels each using the Design Expert software (Version 7.1), wherein 12 experimental runs were generated and executed in a randomized manner. The experimental design matrix for running the experiments is shown in Table 3.

For statistical analysis of the design, ANOVA and coefficients of quadratic equation were considered for both the responses viz particle size and entrapment efficiency. The factors and their levels are shown in Table 4.2.

Table 4.2: Factors and their respective levels for Plackett Burman design

| Factors   | Units  | Levels |      |
|---|--------|--------|------|
|   |        | Low    | High |
| Drug amount ( $X_1$ )                           | mg     | 2      | 5    |
| Polymer amount ( $X_2$ )                        | mg     | 20     | 50   |
| pH of aqueous phase( $X_3$ )                    |        | 4.5    | 8    |
| Incubation time ( $X_4$ )                       | hr     | 3      | 24   |
| Rate of addition of desolvating agent ( $X_5$ ) | ml/min | 0.25   | 0.5  |
| Speed of stirring ( $X_6$ )                     | RPM    | 300    | 600  |

The values for the levels were determined based on preliminary experiments.

Table 4.3: Design Plan for Plackett-Burman Design

| Batch Code | Factors                    |                               |                               |                                |  |                                   |
|------------|----------------------------|-------------------------------|-------------------------------|--------------------------------|--|-----------------------------------|
|            | Drug amount (mg) ( $X_1$ ) | Polymer amount (mg) ( $X_2$ ) | pH of aqueous phase ( $X_3$ ) | Incubation time (hr) ( $X_4$ ) | Rate of addition of desolvating agent (ml/min) ( $X_5$ ) | Speed of stirring (RPM) ( $X_6$ ) |
| PB1        | 2                          | 50                            | 8                             | 24                             | 0.25   | 600                               |
| PB2        | 2                          | 50                            | 4.5                           | 24                             | 0.5  | 600                               |
| PB3        | 2                          | 20                            | 4.5                           | 3                              | 0.25   | 600                               |
| PB4        | 5                          | 50                            | 4.5                           | 3                              | 0.25   | 300                               |
| PB5        | 2                          | 20                            | 8                             | 3                              | 0.5  | 300                               |
| PB6        | 5                          | 20                            | 8                             | 24                             | 0.5  | 600                               |
| PB7        | 5                          | 50                            | 4.5                           | 24                             | 0.5  | 300                               |
| PB8        | 2                          | 20                            | 4.5                           | 24                             | 0.25   | 300                               |
| PB9        | 5                          | 20                            | 4.5                           | 3                              | 0.5  | 600                               |
| PB10       | 2                          | 50                            | 8                             | 3                              | 0.5  | 300                               |
| PB11       | 5                          | 20                            | 8                             | 24                             | 0.25   | 300                               |
| PB12       | 5                          | 50                            | 8                             | 3                              | 0.25   | 600                               |

#### 4.4.2.3 Optimization of Galantamine hydrobromide nanoparticles using Box–Behnken Design (Yerlikaya et al., 2013)

After assessing the critical formulation and process variables using Plackett Burman Design, further optimization of the formulation was done by selecting the Box-Behnken Design (Design Expert, Ver 7.1). Here, a three-factor three-level design matrix was applied for optimization of Galantamine hydrobromide nanoparticles, leading to 17 experiments. The levels were assigned the same values as in Plackett Burman Design. Also, the experiment runs were taken in a randomized manner to minimize associated errors.

Three variables out of the six variables studied in Plackett Burman Design were found to be statistically insignificant towards the response variables; particle size and entrapment efficiency. Therefore their values were fixed and not included in the optimization by Box-Behnken Design (Table 4.4).

Table 4.4: Fixed Process and Formulation Parameters for Box-Behnken Design

| <b>Parameter</b>                               | <b>Fixed level</b> |
|--|--------------------|
| Drug amount (mg)                               | 5                  |
| pH of aqueous phase                            | 8                  |
| Rate of addition of desolvating agent (ml/min) | 0.25               |

The factors and their three levels are shown in Table 4.5 and the design matrix for Box Behnken Design can be viewed in Table 4.6

Table 4.5: The factors and their levels for Box- Behnken Design

| Factor                      | Level |        |     |
|-----------------------------|-------|--------|-----|
|                             | High  | Medium | Low |
| Speed of stirring (RPM) [A] | 600   | 450    | 300 |
| Polymer amount (mg) [B]     | 20    | 35     | 50  |
| Incubation time (hr)[C]     | 5     | 4      | 3   |

Table 4.6: Experimental Plan for Box-Behnken Design

| Batch code | Speed of stirring (RPM) [A] | Polymer amount (mg) [B] | Incubation between drug and polymer (hr)[C] |
|------------|-----------------------------|-------------------------|---|
| BB 1       | 450                         | 50                      | 3   |
| BB2        | 450                         | 20                      | 5   |
| BB3        | 450                         | 35                      | 4.5   |
| BB4        | 600                         | 35                      | 5   |
| BB5        | 450                         | 35                      | 4.5   |
| BB6        | 450                         | 35                      | 4.5   |
| BB7        | 300                         | 35                      | 5   |
| BB8        | 300                         | 20                      | 4.5   |
| BB9        | 600                         | 20                      | 4.5   |
| BB10       | 600                         | 35                      | 3   |
| BB11       | 450                         | 20                      | 3   |
| BB 12      | 450                         | 35                      | 4.5   |
| BB13       | 450                         | 50                      | 5   |
| BB14       | 600                         | 50                      | 4.5   |
| BB15       | 450                         | 35                      | 4.5   |
| BB16       | 300                         | 35                      | 3   |
| BB17       | 300                         | 50                      | 4.5   |

### Optimization Data Analysis

Various RSM (Response Surface Methodology) computations for the current optimization study were performed employing Design Expert® software (version 7.0.7.1, Stat-Ease Inc, Minneapolis, USA). Quadratic models including interaction and quadratic terms were generated for the response variable using multiple regression analysis (MLRA) approach. The general form of MLRA model is represented as equation.

$$Y = b_0 + b_1A + b_2B + b_3C + b_{12}AB + b_{13}BC + b_{23}AC + b_{12}A^2 + b_{22}B^2 + b_{32}C^2 + b_{123}ABC \dots\dots\dots(4.1)$$

Where  $b_0$  is the intercept representing the arithmetic average of all quantitative outcomes of 17 runs;  $b_{ij}$  are the coefficients computed from the observed experimental values of Y; and A, B and C are the coded levels of the independent variable(s). The terms AB and  $X_{i2}$  ( $i=1$  to 3) represents the interaction and quadratic terms, respectively. The main effects (A, B and C) represent the average result of changing one factor at a time from its low to high value. The interaction terms (ABC) show how the response changes when three factors are simultaneously changed. The polynomial terms (AB, BC, and AC) are included to investigate nonlinearity. The polynomial equation was used to draw conclusions after considering the magnitude of coefficients and the mathematical sign it carries, i.e., positive or negative. A positive sign signifies a synergistic effect, whereas a negative sign stands for an antagonistic effect.

The effects of different levels of independent variables on the response parameters were predicted from the respective response surface plots. A FM equation was established after putting the values of regression coefficients of entrapment efficiency and particle size.

The predicted values were calculated by using the mathematical model based on the coefficients of the model and the predicted values along with their observed values were recorded along with percentage of error obtained when predicted value and observed values were compared. Statistical validity of the polynomials was established on the basis of ANOVA provision in the Design Expert ®software. Level of significance was considered at  $p < 0.05$ . F-Statistic was applied on the results of

analysis of variance (ANOVA) of full model and reduced model to check whether the non-significant terms can be omitted or not from the FM (Bolton and Bon; 1997). The best fitting mathematical model was selected based on the comparisons of several statistical parameters including the coefficient of variation (CV), the multiple correlation coefficient ( $R^2$ ), adjusted multiple correlation coefficient (adjusted  $R^2$ ). For simultaneous optimization of particle size and entrapment efficiency, desirability function (multi-response optimization technique) was applied and total desirability was calculated using Design Expert software (version 7.0.7.1). A check point analysis was performed to confirm the utility of the multiple regression analysis and established contour plots in the preparation of Galantamine HBr loaded nanoparticles. Results of desirability criteria, check point analysis and normalized error were considered to select the formulation with lowest particle size and highest entrapment efficiency.

### **Contour Plots**

Contour plots are diagrammatic representation of the values of the responses that help in explaining the relationship between independent and dependent variables. Various contour plots were generated between variables under consideration studied in the design of experiments.

### **Response Surface Plots**

To understand the main and the interaction effects of two variables, response surface plots were used as a function of two factors at a time maintaining all other factors at fixed levels (Mak, Yap, & Teo, 1995). These plots were obtained by calculating the values taken by one factor where the second varied (from -1 to 1 for instance) with constraint of a given Y value. The yield values for different levels of variables could also be predicted from the respective response surface plots.

### **Check Point Analysis**

A check point analysis was performed to confirm the utility of the established contour plots and reduced polynomial equation in the preparation of NPs. Values of independent variables (A and B) were taken from three check points on contour plots plotted at fixed levels of -1, 0 and 1 of C and the values of particle size (Y1) and entrapment efficiency (Y2) were calculated by substituting the values in the reduced

polynomial equation. Galantamine hydrobromide loaded NPs were prepared experimentally by taking the amounts of the independent variables (A and B). Each batch was prepared three times and mean values were determined. Difference in the predicted and mean values of experimentally obtained entrapment efficiency and particle size was compared by using student's 't' test.

**Desirability Criteria**

For simultaneous optimization of particle size and entrapment efficiency, desirability function (multi-response optimization technique) was applied and total desirability was calculated using Design Expert software (version 7.0.7.1). The desirability lies between 0 and 1 and it represents the closeness of a response to its ideal value. The total desirability is defined as a geometric mean of the individual desirability for particle size and entrapment efficiency (Derringer and Suich; 1980).

$$D = (dPS \times dEE)^{1/2} \dots\dots\dots(4.2)$$

Where, *D* is the total desirability, *dEE* and *dPS* are individual desirability for EE and PS. If both the quality characteristics reach their ideal values, the individual desirability is 1 for both. Consequently, the total desirability is also 1. Our optimization criteria included PS of less than 200 nm and maximum EE.

**Normalized Error Determination**

The quantitative relationship established by MRA was confirmed by evaluating experimentally prepared Galantamine HBr loaded NPs. PS and EE predicted from the MRA were compared with those generated from prepared batches of check point analysis using normalized error (NE). The equation of NE is expressed as follows:

$$NE = [\sum\{(Pre - Obs)/Obs^2\}]^{1/2} \dots\dots\dots(4.3)$$

where, Pre and Obs represents predicted and observed response, respectively.

The quadratic equations were generated for each response viz; particle size (*Y*<sub>1</sub>) and entrapment efficiency (*Y*<sub>2</sub>). From these equations, the formulation and process variables that contributed critically to achieve the targeted response could be identified. Additionally, ANOVA was applied to understand the significance of the variables and the model as a whole. All these evaluations, along with construction of

contour plots and response surface graphs, led to the optimization of the formulation with respect to particle size ( $Y_1$ ) and entrapment efficiency ( $Y_2$ )

The optimized Galantamine hydrobromide nanoparticle formulation was prepared and tested to evaluate the correlation between the predicted and the actual values of the responses. The optimum formulation was further characterized for its physicochemical properties.

#### **4.5 Lyophilization of Galantamine hydrobromide Loaded Nanoparticles and Optimization of Cryoprotectant (Anhorn, Mahler, & Langer, 2008)**

The optimized nanoparticle formulations needed to be converted to a stable powder product. Different cryoprotectants (Trehalose dehydrate, Mannitol and Sucrose) at different ratio (1:1w/w, 1:2w/w, 1:3w/w) were tried to select the cryoprotectant which showed minimum increment in particle size. Nanoparticulate suspension (2 ml) was dispensed in 10 ml semi-stoppered vials with rubber closures and frozen for 24 h at -80 °C. Thereafter, the vials are lyophilized (Heto Drywinner, Allerod, Denmark) using different cryoprotectants like trehalose, sucrose and mannitol in different concentrations. Finally, glass vials were sealed under anhydrous conditions and stored until being re-hydrated. Lyophilized NPs were re-dispersed in exactly the same volume of distilled water as before lyophilization.

#### **4.6 Characterization of Galantamine hydrobromide loaded Nanoparticles**

##### *4.6.1 Differential Scanning Calorimetry (DSC)*

DSC helps in identifying possible interaction between drug and polymer and the physical changes of the active and excipient during the process of formulation. DSC analyses of Galantamine hydrobromide, BSA, their physical mixtures and the nanoparticulate formulation were performed using a DSC – 60 instrument (Shimadzu, Japan). Indium was used for internal calibration. The samples were loaded separately into aluminum pans and hermetically sealed. An empty pan was used as reference. The

samples were scanned from 30 °C to 240 °C at a scanning rate of 20°C/min. Nitrogen gas was used for purging the sample holders at a flow rate of 50 mL/min.

#### 4.6.2 X – Ray Diffraction (XRD)

XRD was performed to understand the physical state of BSA and Galantamine hydrobromide before and after their incorporation into the formulation. Additionally, it provided information on physical characteristics of Galantamine hydrobromide after its interaction with BSA during formulation of nanoparticles. Powder X - ray diffraction (PXRD) pattern were recorded using X ray diffractometer (Panalytical's Xpert Pro, Netherlands) using Cu  $k_2\alpha$  rays with a voltage of 45 kV and a current of 40mA in a flat plate  $\theta/2\theta$  geometry, over  $2\theta$  ranges between 5-70° and signals were collected for 20 min. A sample equivalent to 60 mg was placed in the sample holder groove and tightly packed.

#### 4.6.3 Entrapment Efficiency

For entrapment efficiency, the dispersion of Galantamine hydrobromide loaded nanoparticles were centrifuged 35,000 RPM, at 4° C for 30 minute (Optima L-100XP, Beckmann, USA). The supernatant was separated from the formed pellet and analyzed for free GAL by UV (UV 1800, Shimadzu, Japan) at 289 nm against standard calibration curve. The drug entrapment was defined as the percentage of entrapped Galantamine hydrobromide in relation to the initial amount of drug.

#### 4.6.4 Particle Size

The size and polydispersity index of the nanoparticles were determined using Malvern Zetasizer NanoSeries nano-ZS (Malvern Instruments Limited, Worcestershire, UK). Each sample was diluted ten times with filtered distilled water to avoid multi scattering phenomena and placed in a disposable sizing cuvette. Polydispersity index was studied to determine the narrowness of the particle size distribution. The size analysis of a sample consisted of 3 measurements, and the results are expressed as mean size  $\pm$ SD.

#### 4.6.5 Zeta Potential

Zeta potential was measured using a Zetasizer (NanoSeries nano-ZS Malvern Instruments Limited, Worcestershire, UK). Each sample was suitably diluted with filtered distilled water and placed in a disposable zeta cell. Zeta limits ranged from -200 to +200 mV. The electrophoretic mobility ( $\mu\text{m}/\text{sec}$ ) was converted to zeta potential by in-built software using Helmholtz-Smoluchowski equation. Average of 3 measurements of each sample was used to derive zeta potential

#### 4.6.5 Transmission Electron Microscopy

The morphology, structure and size of Galantamine hydrobromide nanoparticles were observed through Transmission Electron Microscope (TEM) (Tecnai 20, Phillips, Holland) operating at an accelerating voltage of 200 kV, providing magnification upto 7,50,000 X. The suspension of nanoparticles was deposited on a 200 mesh form (Johansson, 1997)var – coated copper grid and scanned at various magnifications.

#### 4.6.6 Atomic Force Microscopy(Moribe et al., 2012)

To understand the topography of the Galantamine hydrobromide loaded nanoparticles, Atomic Force Microscope (AFM) (Bruker Dimension Icon, USA) equipped with ScanAsyst Software was used. Sample was loaded on a Mica plate (MUSCOVITE MICA, V- 1 quality,USA) and spread uniformly on its surface. The mica plate was stored in a dessicator without dessicant for 15 min to immobilize them onto the surface. This plate was then placed under the microscope, which was placed on a vibration free table with an insulation cover. After setting the desired field of vision, the silicon tip cantilever was allowed to oscillate in the tapping mode with a spring constant of approximately 0.05 N/m and a resonance frequency of approximately 37 kHz. The AFM topography image which reflects the topographic features of the surface was obtained from the amplitude change of the cantilever oscillation.

#### 4.6.7 *In vitro* drug release studies (Mufamadi et al., 2013)

*In – vitro* drug release study of Galantamine hydrobromide loaded albumin nanoparticles was accomplished using dialysis bag diffusion technique. The studies of release of Galantamine hydrobromide were performed in phosphate buffer saline (PBS) pH 7.4. The aqueous nanoparticulate dispersion equivalent to 4 mg of Galanamine hydrobromide was placed in a dialysis bag (CelluSep T1, Uptima, U.S.) which had a MWCO of 3500 Da. The dialysis bag was immersed in 50 mL of PBS, which was stirred on a magnetic stirrer (Remi Instruments, India) at 100 rpm and maintained at  $37\pm 2^{\circ}\text{C}$ . The receptor compartment was covered to prevent evaporation of release medium. Samples were withdrawn at regular time intervals, and the same volume was replenished to maintain sink conditions. The samples were measured for Galantamine Hydrobromide by UV – Visible Spectroscopy (UV 1800, Shimadzu, Japan). All the experiments were performed in triplicate, and the average values were recorded. Galantamine hydrobromide was dissolved in PB (pH = 7.4) was used as a control

#### 4.6.8 *Ex vivo* drug diffusion studies

*Ex – vivo* drug diffusion studies were performed using sheep nasal mucosa. The mucosa was obtained from an authorized abattoir in Vadodara. The turbinates were fully exposed by a longitudinal incision through the nose. The turbinate mucosa was carefully removed from the underlying bone by cutting with a haemostatic forceps and pulling the mucosa off. The excised tissue was stored directly on ice during transportation to the laboratory. This tissue was then mounted on the upper chamber of a Franz diffusion cell. The receptor chamber was filled with 50 mL PBS (pH = 7.4). The aqueous nanoparticulate dispersion equivalent to 4 mg of Galanamine hydrobromide was placed on the tissue. The receptor chamber was stirred at 100 rpm and maintained at  $37\pm 2^{\circ}\text{C}$ . Samples were withdrawn at regular time intervals, and the same volume was replenished to maintain sink conditions. The samples were measured for Galantamine Hydrobromide by UV – Visible Spectroscopy (UV 1800, shimadzu, Japan). All the experiments were performed in triplicate, and the average

values were taken. Galantamine hydrobromide was dissolved in in PB (pH = 7.4) was used as a control.

## 4.7 Results and Discussion

### 4.7.1 Optimization of blank nanoparticles

The size of nanoparticles is of utmost importance considering nose to brain targeting, hence initial optimization of blank nanoparticles was done keeping particle size as the main criterion.

#### (1) Choice of desolvating agent:

For the purpose of desolvation, the chosen organic solvent should be miscible with water but the drug and polymer should be insoluble in the desolvating agent. Table 4.7 shows the effect of desolvating agent on particle size.

Chloroform and isopropyl alcohol did not to lead proper desolvation and the end product had a gel like appearance. This could be probably due to the ability of bovine serum albumin to bind to chloroform (Johansson, 1997)

Alcohol led to formation of particle size greater than 500 nm may be due to faster desolvation. Acetone provided nanoparticles with smallest particle size ranging from 100 - 200 nm

Hence, acetone was selected as the desolvating agent.

Smaller the particle size, better the chances of brain targeting via the nasal route. Therefore the achieved particle size was suitable for the formulation of brain targeted nanoparticles

Table 4.7: Effect of desolvating agent on particle size.

| <b>Desolvating agent</b> | <b>Particle size (nm) *</b> |
|--------------------------|-----------------------------|
| Chloroform               | No proper desolvation       |
| Isopropyl alcohol        | No proper desolvation       |
| Absolute alcohol         | 542.39 ± 12.36              |
| Acetone                  | 154.31 ± 10.79              |

\* : Studies were done in triplicate.

## (2) Rate of addition of desolvating agent:

The rate at which desolvating agent was added to the aqueous phase plays an important role in determining the particle size of nanoparticles. Table 4.8 shows the effect of rate of addition of desolvating agent on particle size.

The rate of addition of desolvating agent was varied from 1.0 ml/min to 0.25 ml/min. It was observed that as the rate of addition was lowered, the particle size reduced. By further lowering the rate of addition of desolvating agent, the effective concentration of non aqueous to aqueous at that time point would reduce, which in turn would hinder the proper desolvation. Additionally further lowering the rate of addition of desolvating agent would increase the total time required for formulating the nanoparticles.

The rate of addition was not reduced below 0.25 ml/min as the desired particle was achieved.

Hence, the rate of addition of desolvating agent was kept in the range of 0.5 to 0.25 ml/min.

Table 4.8: Effect of rate of addition of desolvating agent on particle size.

| <b>Rate of addition of desolvating agent (ml/min)</b> | <b>Particle size (nm) *</b> |
|---|-----------------------------|
| 1.0 – 0.75  | 411.23 ± 23.47              |
| 0.75 – 0.5  | 261.19 ± 19.11              |
| 0.5 – 0.25  | 119.78 ± 13.77              |

\* : Studies were done in triplicate.

## (3) Bovine serum albumin concentration in the solution:

The concentration of Bovine Serum Albumin was varied from 25 mg/ml to 6.25 mg/ml.

At 25 mg/ml, nanoparticles of larger particle size were formed, mainly due to larger solid content. At 12.5 mg/ml smaller particles were formed in the range of 100 – 200 nm. Similarly, at 6.25 mg/ml very small particles were formed but yield was poor indicating that desolvation did not take place properly may be because of low polymer concentration.

Hence, 12.5 mg/ml was finalized as the Bovine serum albumin concentration in solution.

Table 4.9: Effect of rate of addition of desolvating agent on particle size.

| <b>Bovine serum concentration (mg/mL)</b> | <b>Particle size (nm) *</b> |
|---|-----------------------------|
| 25  | 447.19 ± 16.11              |
| 12.5                                      | 294.14 ± 17.34              |
| 6.5                                       | 123.25 ± 14.68              |

\* : Studies were done in triplicate.

(4) Centrifugation speed for collecting nanoparticles:

For the separation of formed nanoparticles from the aqueous phase, centrifugation was carried at various speeds to the point a distinct pellet was obtained with a clear supernatant.

All the trials were done at 4°C.

At an RPM of 5000 to 25000, there was no separation achieved. Proper separation was achieved at 35000 RPM.

#### 4.7.2 Formulation of Galantamine hydrobromide nanoparticles

There are many reports (Merodio et al., 2001; S. Wagner et al., 2010) on BSA nanoparticles for delivering anti cancer drug. However, its potential use as a carrier for anti Alzheimer drug has been less tread upon. As mentioned earlier, the aim was to prepare nanoparticles with minimum steps and less number of excipients so that it's commercially feasible.

The method chosen was desolvation followed by thermal gelation. This method is simple and produces small nanoparticles with a narrow distribution and very low polydispersity index (Qi et al., 2014). It is a well proven fact that the mean diameter of nanoparticles administered intranasally should be small to encourage uptake by endocytic pathways. In general, nanoparticles of a diameter <200 nm are efficiently internalized by clathrin-mediated endocytosis (Hanafy et al., 2015). Therefore, it's very crucial to control formulation and process parameters for obtaining desired particle size.

### 4.7.3 Preliminary studies for formulation of GAL nanoparticles

The choice of BSA as a polymer for formulation of GAL nanoparticles, served two purposes; first, it being an anionic polymer at alkaline pH, the chances of entrapment of cationic Galantamine increases. Secondly, BSA itself has a stabilizing effect in an aqueous media, it acts as a surface active agent, therefore, there is no requirement of an additional excipient like surfactant to stabilize the nanoparticulate system (Tantra, Tompkins, & Quincey, 2010). Hence, the formulation remains simple, requires minimum excipients and doesn't involve complex steps.

#### 4.7.3.1 Risk Identification and Risk Analysis

Ishikawa diagram (Fish bone analysis) helps in identification of the CQAs of a formulation and also helps in visualizing all the possible risks involved to achieve the CQAs. Here, the CQAs were particle size and entrapment efficiency. Both of these are of great significance when they are correlated with the administration route. Ishikawa diagram for particle size and entrapment efficiency are represented in Figure 4.1 and Figure 4.2 respectively.

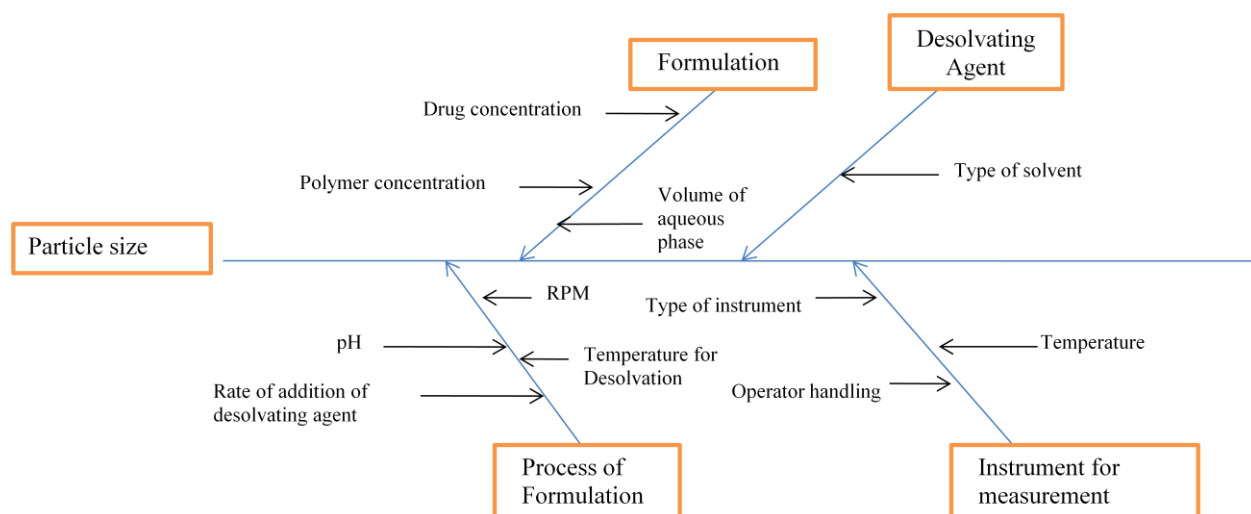


Figure 4.1: Ishikawa diagram to understand the Critical Quality Attributes contributing to particle size.

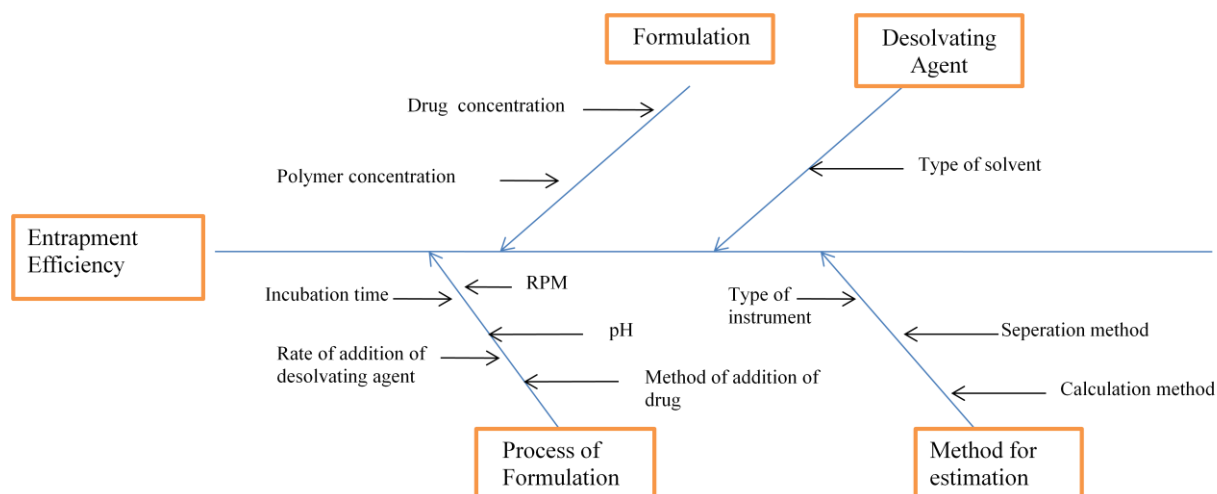


Figure 4.2: Ishikawa diagram for understanding the Critical Quality Attributes contributing to entrapment efficiency.

For intranasal administration to brain, particle size plays a pivotal role in carrying the drug to its target. Their small diameter potentially allows nanoparticles to be transported transcellularly through olfactory neurons to the brain via the various endocytic pathways of sustentacular or neuronal cells in the olfactory membrane. Therefore it was aimed to obtain nanoparticles with size less than 200 nm.

On the other hand, high encapsulation efficiency can help in reducing bulk of formulation to be administered, also avoiding drug wastage during formulation. Hence it was identified as a CQA to be optimized for ensuring high entrapment efficiency.

Additionally, the technique of Failure Mode Effect Analysis (FMEA) was applied to gauge and visualize all the possible failures in the design of the formulation. This was done by means of ranking the failures with the help of RPN.

The RPN was calculated by scoring based on Severity, Detectability and Probability. Severity is a measure of the possible consequences of a failure mode affecting on the safety and efficacy of the final product. Detectability defined that a failure mode can be detected.

These parameters were ranked, wherein 4 was the worst case, 1 was the best and 2 as moderate value. From these parameters, the Risk Priority Number (RPN) was calculated using the formula:

$$RPN = S \times D \times P \dots\dots\dots(4.4)$$

Therefore the maximum value for RPN could be 64 and the minimum value could be 1.

The threshold for RPN was fixed at 48, and any formulation variable or process parameter with an RPN 48 or above was regarded as a potential critical factor. These factors had more potential risk than other factors on affecting the CQAs (Kan et al., 2014). Higher the RPN, higher is the risk and hence should be taken into account while designing a formulation.

The chart demonstrating all the possible risks leading involved in formulation of GAL nanoparticles is shown in Figure 4.3.

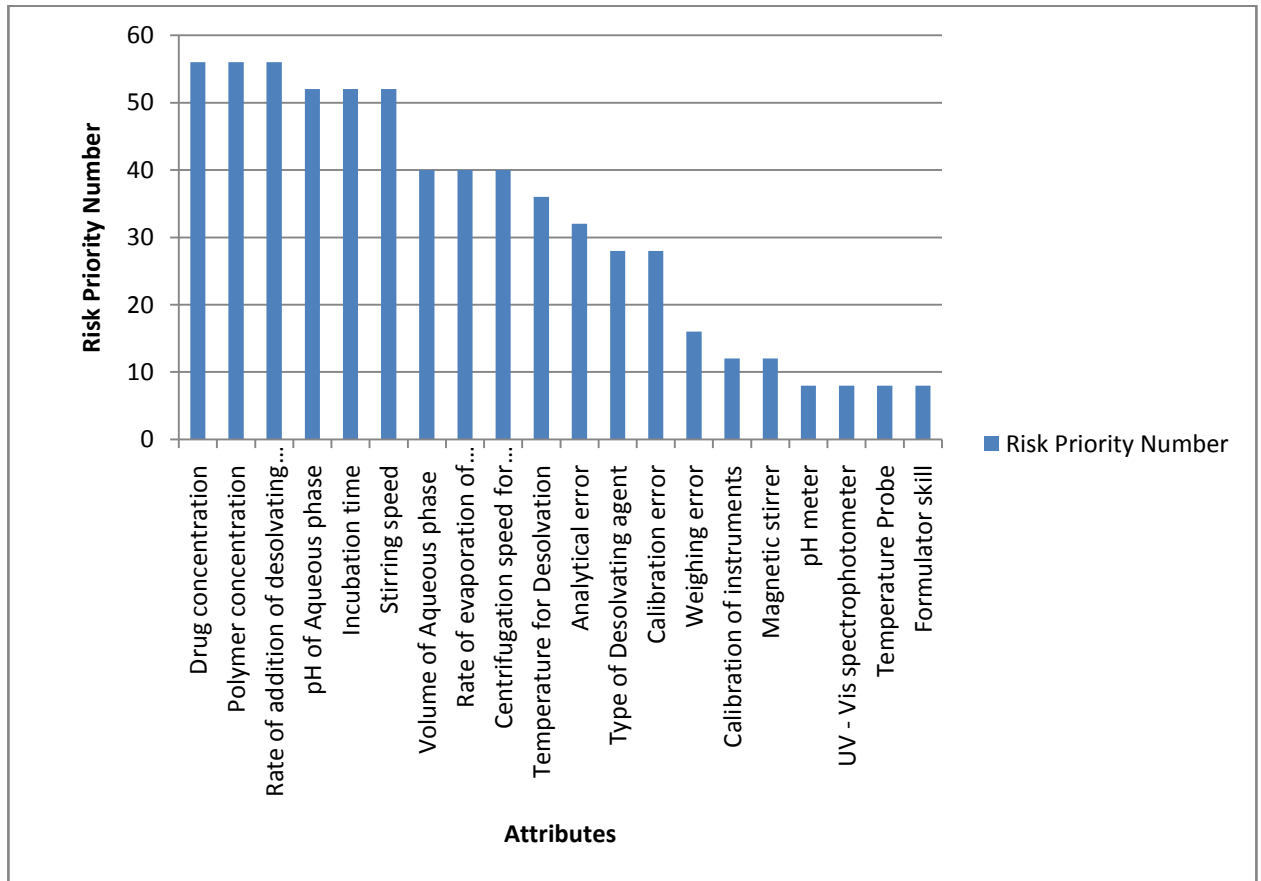


Figure 4.3: Risk Priority Number associated with various attributes contributing to formulation of GAL nanoparticles.

From figure 4.3 it could be seen that drug amount, polymer amount, rate of addition of desolvating agent, pH of aqueous agent, incubation time between drug and polymer and stirring speed had the RPN higher than 48. Hence these factors were considered further for risk assessment and optimization.

#### 4.7.3.2 Risk Analysis by Plackett-Burman Design

Based on the FMEA, statistical analysis of six factors was done by Plackett – Burman Design. The outcome of the design for Particle size ( $Y_1$ ) and Entrapment efficiency ( $Y_2$ ) are shown in Table 4.10.

Table 4.10: Results of responses after Plackett –Burman Design

| <b>Batch Code</b> | <b>Particle Size in nm (<math>Y_1</math>)</b> | <b>Entrapment Efficiency in % (<math>Y_2</math>)</b> |
|-------------------|---|--|
| PB1               | 385.14 ± 7.12                                 | 40.12 ± 3.93   |
| PB2               | 450.12 ± 8.14                                 | 0.16 ± 0.02  |
| PB3               | 234.74 ± 5.36                                 | 2.57 ± 0.17  |
| PB4               | 512.26 ± 8.54                                 | 6.4 ± 0.69   |
| PB5               | 670.89 ± 5.31                                 | 64.12 ± 2.83   |
| PB6               | 280.73 ± 7.06                                 | 24.17 ± 2.32   |
| PB7               | 575.23 ± 6.97                                 | 1.39 ± 0.24  |
| PB8               | 731.49 ± 4.38                                 | 5.17 ± 0.23  |
| PB9               | 300.14 ± 9.13                                 | 3.47 ± 0.13  |
| PB10              | 743.54 ± 11.78                                | 57.96 ± 4.36   |
| PB11              | 845.61 ± 10.46                                | 32.78 ± 1.96   |
| PB12              | 110.22 ± 9.18                                 | 78.56 ± 4.67   |

Table 4.11: Statistical analysis of effect of variables on responses for Plackett-Burman Design

| Factors   | Particle size in nm ( $Y_1$ ) |                | Entrapment Efficiency ( $Y_2$ ) |                |
|---|-------------------------------|----------------|---------------------------------|----------------|
|   | % Contribution                | <i>p</i> Value | % Contribution                  | <i>p</i> Value |
| Drug concentration ( $X_1$ )                    | 4.94                          | 0.1771         | 0.53                            | 0.5983         |
| Polymer concentration ( $X_2$ )                 | 1.16                          | 0.4803         | 2.64                            | 0.2589         |
| pH of aqueous phase ( $X_3$ )                   | 0.76                          | 0.5645         | 11.53                           | 0.0404         |
| Incubation time ( $X_4$ )                       | 6.83                          | 0.1240         | 74.91                           | 0.0006         |
| Rate of addition of desolvating agent ( $X_5$ ) | 0.57                          | 0.6167         | 0.20                            | 0.0443         |
| Speed of stirring ( $X_6$ )                     | 75.72                         | 0.0017         | 0.34                            | 0.812          |

Table 4.11 represents the statistical treatment given to each variable to understand its effect on the responses.

For particle size ( $Y_1$ ), the percent contribution of speed of stirring, incubation time between the drug and polymer, drug concentration and polymer concentration was the maximum. The *p* value for the model was 0.0215, the *F* value was 7.49, and the  $R^2$  was 0.89. Also, the model had fewer signal to noise ratio. The *p* value for incubation time, drug amount and polymer amount was greater than 0.05 and hence was not significant in the designed model. Therefore, RPM of magnetic stirrer was singled out as the factor contributing to smaller particle size.

For entrapment efficiency ( $Y_2$ ), the contribution of incubation time, pH of aqueous phase and polymer amount was highest. The *p* value for model was 0.0062, whereas *F* value was 10.57 which indicated the model was highly significant. The pH of the

aqueous phase, incubation time and rate of addition of desolvating agent were significant variables for entrapment efficiency. The pH of aqueous phase solution, when kept at an alkaline side resulted in better entrapment since the isoelectric point of BSA is pH 4.5. Hence, at alkaline pH, the anionic polymer reacted with the cationic drug to give high entrapment. Similarly, the time for which the drug and polymer were in contact prior to desolvation also plays an important role in improving the entrapment efficiency. The entrapment efficiency increased till 4-5 hours of incubation.

Through preliminary studies for formulation, polymer amount, drug amount, rate of addition of desolvating agent, pH of the aqueous phase, incubation time were some of the factors that were found to influence the formation of Galantamine hydrobromide nanoparticles.

After the risk assessment with Plackett-Burman Design, the pH of the aqueous phase and rate of addition of desolvating agent was kept constant for optimization, since they were not as significant as incubation time for entrapment efficiency. Additionally, polymer amount was taken ahead for optimization, as this factor had a contribution in both the responses.

#### 4.7.3.3 Optimization by Box-Behnken Design

After determining the statistically significant and important formulation and process variables by Plackett–Burman design, a three-factor, three-level Box–Behnken design was applied to precisely understand the impacts of RPM of magnetic stirrer (A), polymer amount (B), and incubation time (C) on particle size and encapsulation efficiency of GAL nanoparticles. The results of experimental runs are given in Table 4.12.

Table 4.12: Results of responses for Box-Behnken Design

| Batch Code  | Particle Size in nm<br>(Y <sub>1</sub> ) | Entrapment<br>Efficiency in % (Y <sub>2</sub> ) |
|-------------|--|---|
| BB 1        | 300.52 ± 7.05                            | 20.14 ± 2.63                                    |
| BB2         | 426.51 ± 9.86                            | 15.23 ± 1.89                                    |
| BB3         | 380.83 ± 4.80                            | 39.45 ± 2.35                                    |
| BB4         | 215.76 ± 2.09                            | 22.19 ± 1.54                                    |
| BB5         | 394.19 ± 4.50                            | 41.23 ± 1.51                                    |
| BB6         | 400.73 ± 7.84                            | 43.57 ± 2.29                                    |
| BB7         | 540.17 ± 8.08                            | 19.27 ± 3.38                                    |
| BB8         | 641.23 ± 7.14                            | 28.78 ± 1.34                                    |
| BB9         | 348.21 ± 4.95                            | 25.14 ± 1.89                                    |
| BB10        | 430.63 ± 6.90                            | 18.59 ± 1.95                                    |
| BB11        | 519.47 ± 6.96                            | 14.29 ± 2.37                                    |
| BB 12       | 379.36 ± 2.50                            | 44.87 ± 3.70                                    |
| BB13        | 386.1 ± 2.32                             | 22.74 ± 2.66                                    |
| <b>BB14</b> | <b>114.98 ± 1.16</b>                     | <b>78.23 ± 2.04</b>                             |
| BB15        | 357.66 ± 4.29                            | 36.88 ± 1.13                                    |
| BB16        | 682.91 ± 7.89                            | 22.39 ± 1.56                                    |
| BB17        | 756.38 ± 6.04                            | 72.12 ± 2.29                                    |

From table 4.12 it could be seen that the particle size of nanoparticles prepared with lower RPM was found to be more than 300 nm, which was not desirable for intranasal administration. However, higher RPM resulted into nanoparticles with particles less than 200 nm, the minimum being about 110 nm.

During desolvation, higher RPM generated turbulence which prevented the formation of larger particles, as well as aggregation of particles (Patel, Poddar, Sawant, & 2014). This in turn helped to maintain the particle size within a narrow distribution range.

Also, if the incubation time is very high, there are chances of greater ionic interaction between drug and polymer, causing formation of larger particles. On the other hand, if the incubation time is very low, the ionic interaction might not be sufficient enough for proper particle formation. Moreover, drug entrapment might be low.

The quadratic equation obtained for the design with respect to particle size was:

$$Y_1 = 362.56 - 188.89A - 47.18B - 45.62C - 87.09AB - 18.03AC + 44.63BC + 80.92A^2 + 21.71B^2 + 23.87C^2 \dots\dots\dots(4.5)$$

Equation 4.5 shows that all three factors had a negative influence on size that is, size decreased with increase in these variables. The most significant factor contributing to smaller particle size was the RPM of magnetic stirrer, followed by polymer concentration and incubation time.

Moreover, interaction terms AB and AC were also negative but a positive interaction was observed between B (polymer concentration) and C (incubation time).

In case of entrapment efficiency, polymer concentration was the most critical variable (Table 4.12).

Greater polymer amount improves its probability of surrounding the drug, increasing the drug entrapment. However, the polymer amount should be optimum so that the size of the nanoparticles is also under control.

The quadratic equation obtained for the design with respect to entrapment efficiency was:

$$Y_2 = 47.13 + 0.19A + 13.72B + 0.50C + 2.44AB + 1.68AC + 0.415BC + 3.22A^2 + 0.71B^2 - 29.74C^2 \dots\dots\dots(4.6)$$

Equation 4.6 indicates that though all three factors had positive influence on entrapment efficiency, polymer concentration (B) contributed most significantly to entrapment efficiency.

Moreover, positive interactions were seen between all three factors; meaning, higher the value of these coefficients, higher would be the entrapment. The model was evaluated by coefficient of determination ( $R^2$ ). The  $R^2$  values were 0.89 and 0.79 for particle size and entrapment efficiency respectively, indicating that the model fitted significantly and also that a large amount of variance in the response was explained by the model (89 % for particle size and 79% for entrapment efficiency).

ANOVA was applied for models tested for particle size and entrapment efficiency and the  $p$  values were 0.0115 and 0.0485 respectively indicating the suitability to predict the effect of variables on the responses.

Table 4.13: Statistical analysis of effect of variables on responses for Box-Behnken Design

| Factors                   | Particle size in nm ( $Y_1$ ) |           | Entrapment Efficiency ( $Y_2$ ) |           |
|---------------------------|-------------------------------|-----------|---------------------------------|-----------|
|                           | Sum of Squares                | $p$ Value | Sum of squares                  | $p$ Value |
| Speed of Stirring (A)     | 285431.7                      | 0.0003    | 0.316012                        | 0.9689    |
| Polymer concentration (B) | 17807.62                      | 0.1507    | 1506.731                        | 0.0268    |
| Incubation time(C)        | 16652.21                      | 0.1627    | 2.02005                         | 0.0214    |
| AB                        | 30342.16                      | 0.0732    | 23.76563                        | 0.7362    |
| AC                        | 1300.684                      | 0.6760    | 11.2896                         | 0.8160    |
| BC                        | 7969.133                      | 0.3163    | 0.6889                          | 0.9541    |
| $A^2$                     | 27576.68                      | 0.0847    | 43.75816                        | 0.6487    |
| $B^2$                     | 1984.751                      | 0.6069    | 2.145007                        | 0.9191    |
| $C^2$                     | 2400.82                       | 0.5722    | 3725.013                        | 0.0032    |

Table 4.13 shows that, the  $p$  value for stirring speed is 0.003, signifying its important role in reducing the particle size. Also, the  $p$  value for the incubation time is less than 0.05, and hence is significant for entrapment efficiency. Proper incubation time allows proper ionic interaction between the drug and polymer. Higher the incubation, higher is the entrapment. However as the incubation time also affected the particle size, it had to be optimized to balance entrapment and size.

To have a meticulous estimation of various factors on the responses, the significant variables affecting particle size and encapsulation efficiency were visually presented in contour and response surface plots (Figure 4.4 and Figure 4.5 respectively).

Contour plots are a graphical representation of the relationship between three variables in two dimensions. These can be very helpful in illustrating the complete picture of the effect of two independent variables simultaneously (interactions) on the third variable (dependant variable) (Verma, Lan, Gokhale, & Burgess, 2009).

The contour plot for particle size can be seen in Figure 4.4, wherein the incubation time was set at the medium level of 4.5 hours and the other factors were varied. The incubation time was kept fixed since its value was least in equation 4.5. Polymer concentration and speed of stirring were varied. Here, both the varying factors had an inverse relation with particle size.

The contour plot for entrapment efficiency is shown in Figure 4.5. The speed of stirring was set at a maximum value of 600 RPM. A direct relation was observed between both the factors; incubation time and polymer amount on the response, that is entrapment efficiency.

The contour plots aided in providing an idea on what should be the values of varying parameters to achieve a particular particle size.

Similarly, considering other factors, the process can be optimized to achieve the desired product. Various contour plots can be generated between other variables studied in the design of experiments.

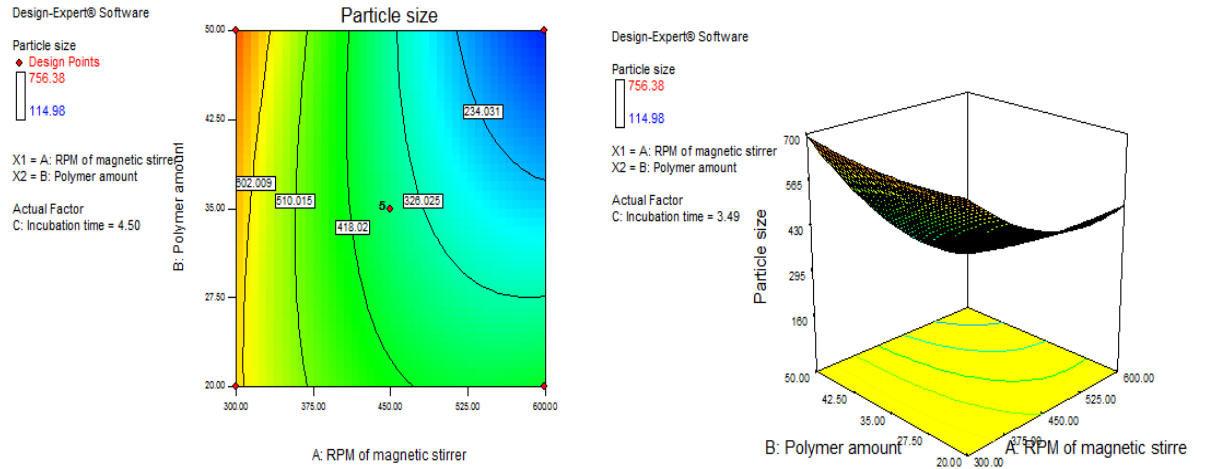


Figure 4.4: Response surface plot and contour plot for the significant variables on particle size

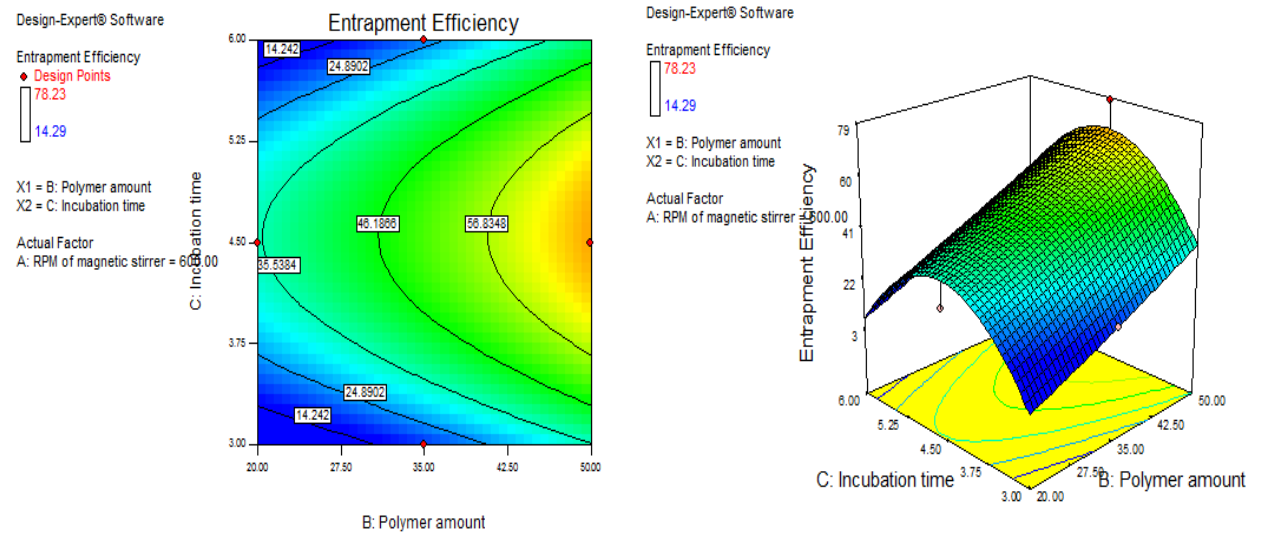


Figure 4.5: Response surface plot and contour plot for the significant variables on entrapment efficiency.

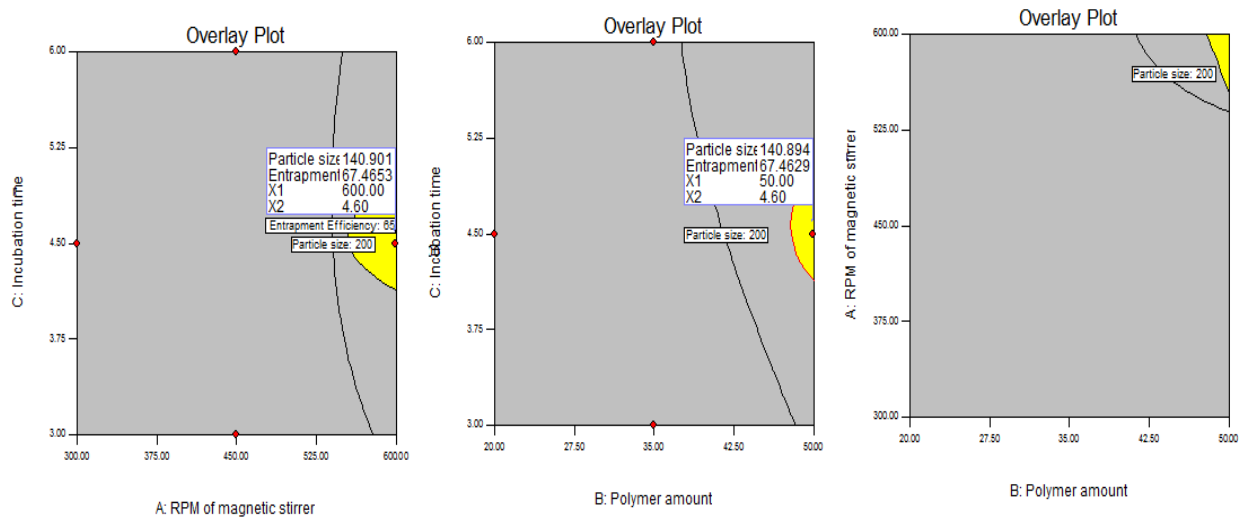


Figure 4.6: Design space for GAL nanoparticles through overlay contour plots.

The design space for Galantamine hydrobromide nanoparticles was established targeting particle size lower than 140 nm and encapsulation efficiency higher than 75 %. For this, overlaid contour plots including both the responses were constructed, as seen in Figure 4.6.

The overlaid contour plots were observed by superimposing the critical response contours of a contour plot. This resulted in the yellow region in Figure 4.6, describing an area of design space with feasible response values and grey region describing an area where response values did not fit the quality product criteria (B. Shah, Khunt, Bhatt, Misra, & Padh, 2015). For instance, in Figure 4.6a, to achieve a particle size of 140.92 nm and entrapment efficiency of 67.46 % during formulation, the RPM of stirring should be 600 and the incubation time should be kept upto 4.6 hours.

#### 4.7.4 Characterization of Galantamine hydrobromide nanoparticles

##### 4.7.4.1 Differential Scanning Calorimetry (DSC)

These studies are done before initiation of formulation of any dosage form to gauge the degree of compatibility between the excipients to be used and drugs.

DSC provides details regarding the physical and energy state of a substance. Through DSC, it is possible to determine the physical state of drug substance in nanoparticles.

The results of DSC are shown in Figure 4.7. Pure Galantamine hydrobromide (4.7b) showed a sharp exothermic peak at 280 °C, representing its melting point as well as confirming its crystalline nature. The physical mixture of BSA and Galantamine hydrobromide showed characteristic peaks of both BSA and Galantamine hydrobromide (4.7c). The DSC of Galantamine hydrobromide nanoparticles(4.7d) did not show any peak at the melting point of Galantamine hydrobromide demonstrating its encapsulation into polymer matrix and also the possibility of it being in amorphous state. While formulating a dosage form, it is preferred that the drug in the formulation is amorphous, resulting in better dissolution, absorption and bioavailability (Qi et al., 2014).

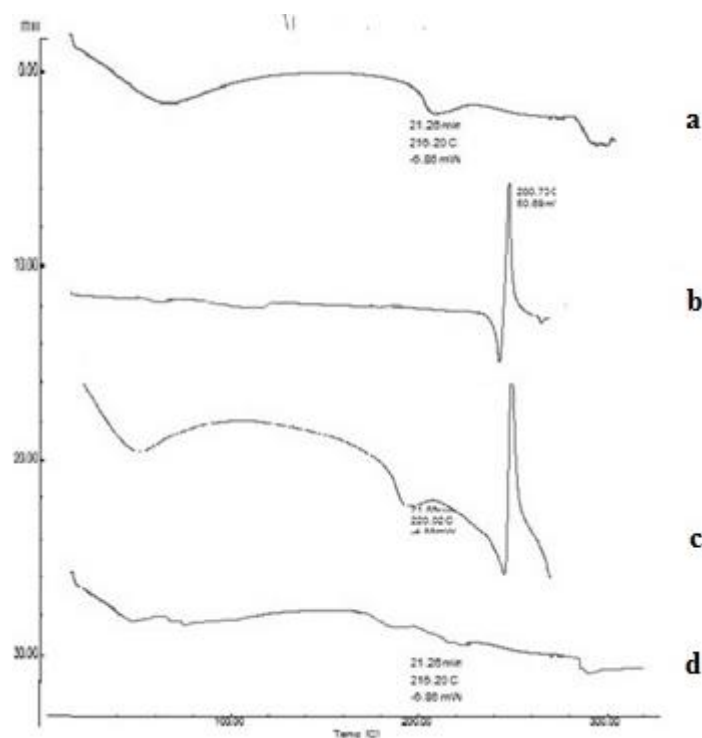
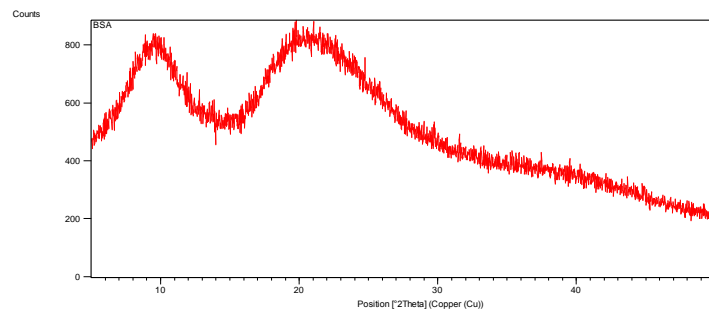


Figure 4.7: DSC of (a) BSA (b) Pure Galantamine hydrobromide (c) Physical mixture of Galantamine hydrobromide and BSA (d) Galantamine hydrobromide nanoparticles.

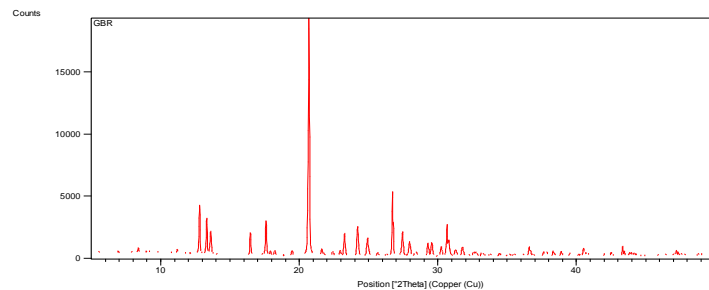
#### 4.7.4.2 X – ray Diffraction (XRD)

As seen in Figure 4.8. BSA showed a halo pattern confirming its amorphous nature. The XRD pattern of Galantamine hydrobromide showed sharp 2 $\theta$  peak at 20.67 ° with an area under the peak of 2200.83. Sharp and distinct peaks in a XRD pattern denotes

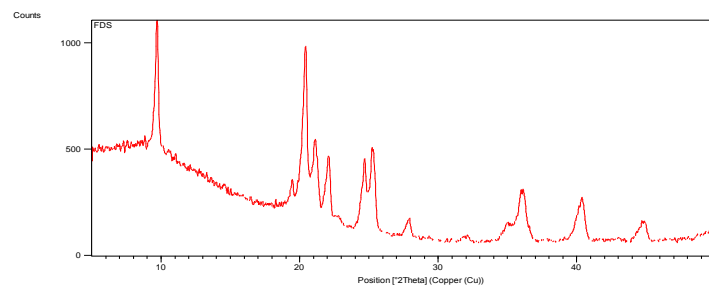
that the substance is crystalline in nature. The diffraction pattern of Galantamine hydrobromide nanoparticles showed diminished peaks of the drug with an area under peak of 147.54 which suggested the presence of crystal particles. However, since the value of area under peak for nanoparticles was substantially lower than the one for pure drug, it could be said that the drug may exist in mixed form, that is the crystalline nature is retained to some extent. Thermograms of DSC does not reflect this since crystallinities of under 2% cannot generally be detected by this method. (J. Kreuter, Feste Dispersionen, in: J. Kreuter, C. D. Herzfeldt, 1999).



a



b



c

Figure 4.8: XRD of (a) BSA (b) Pure Galantamine hydrobromide (c) Galantamine hydrobromide nanoparticles.

#### 4.7.4.3 Zeta potential

Zeta potential is closely related to the stability of the nanoparticle system. The same type of surface charge could provide repulsion among the nanoparticles, maintaining an appropriate particle density and stability (Qi et al., 2014). Here, a negative zeta potential was observed for Galantamine hydrobromide nanoparticles, ranging from  $-13 \text{ mV} \pm 0.25$  to  $-11 \text{ mV} \pm 0.32$ .

The zeta potential of blank BSA nanoparticles ranged from  $-18 \text{ mV} \pm 0.16$  to  $-23 \text{ mV} \pm 0.30$ . Thus, the Galantamine hydrobromide loaded nanoparticles had lower zeta potential than the blank nanoparticles indicating interaction between the negatively charged BSA and the positively charged drug, thereby reducing the zeta potential.

This low negative zeta potential along with small particle size was thought to be desirable prerequisites for good brain uptake (Fornaguera et al., 2015).

#### 4.7.4.4 Transmission Electron Microscopy

Figure 4.9 shows that the Galantamine hydrobromide nanoparticles were spherical, uniform in size and had size less than 200 nm.

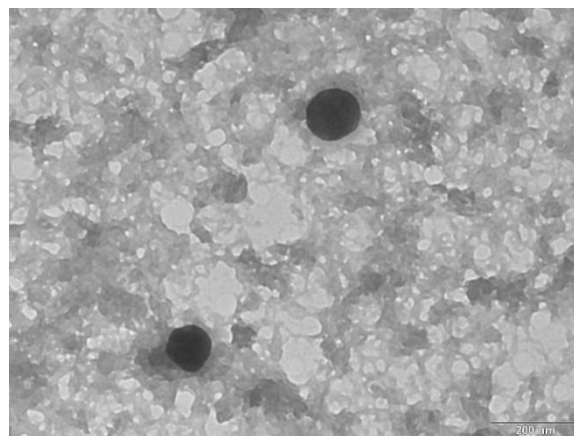


Figure 4.9: TEM of Formulation Code BB14

#### 4.7.4.5 Atomic Force Microscopy

Figure 4.10 shows the three dimensional AFM topography of Galantamine hydrobromide nanoparticles.

The surface was smooth with few undulations, which might suggest the presence of Galantamine hydrobromide adsorbed on the BSA surface during the process of ionic interaction between Galantamine hydrobromide and BSA. This result is in line with the observations from zeta potential study wherein the Galantamine hydrobromide nanoparticles had lower zeta potential than blank BSA nanoparticles, suggesting some level of interaction between BSA and Galantamine hydrobromide.

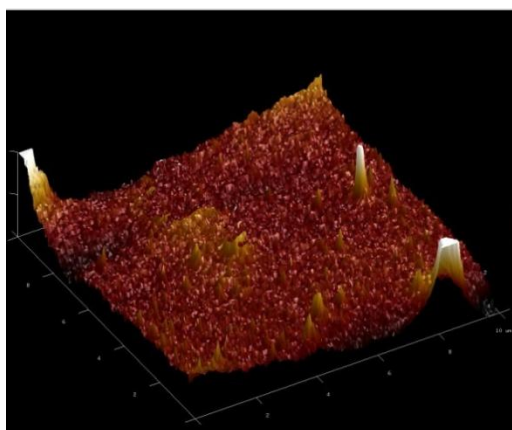


Figure 4.10: Three dimensional AFM topography of Galantamine hydrobromide nanoparticles.

#### 4.7.4.6 *In vitro* drug release studies

*In vitro* drug release studies from plain drug solution and Galantamine hydrobromide loaded nanoparticles is shown in Figure 4.11. The plain drug solution released completely from the dialysis membrane in 1h. On the other hand,  $99.67 \pm 4.78\%$  Galantamine hydrobromide was released in 8 h (Table 4.14). The drug release from nanoparticles followed the biphasic model, with an initial burst attributed to the drug-

associated near-particle surface which may have got desorbed upon contact with the dissolution medium (Seju, Kumar, & Sawant, 2011).

Table 4.14: *In vitro* drug release data for plain drug solution and Galantamine hydrobromide loaded nanoparticles by using dialysis technique

| Time (hour) | Plain drug solution<br>% Drug release $\pm$ SD | Nanoparticles<br>% Drug release $\pm$ SD |
|-------------|--|--|
| 0           | 0  | 0  |
| 0.25        | 35.14 $\pm$ 3.68                               | 1.14 $\pm$ 0.32                          |
| 0.5         | 75.16 $\pm$ 5.71                               | 10.28 $\pm$ 2.58                         |
| 1           | 99.17 $\pm$ 4.44                               | 38.55 $\pm$ 3.78                         |
| 2           |  | 36.22 $\pm$ 4.55                         |
| 3           |  | 45.98 $\pm$ 3.83                         |
| 4           |  | 58.31 $\pm$ 4.11                         |
| 5           |  | 79.14 $\pm$ 2.97                         |
| 6           |  | 88.53 $\pm$ 3.19                         |
| 7           |  | 95.10 $\pm$ 3.24                         |
| 8           |  | 99.67 $\pm$ 3.26                         |

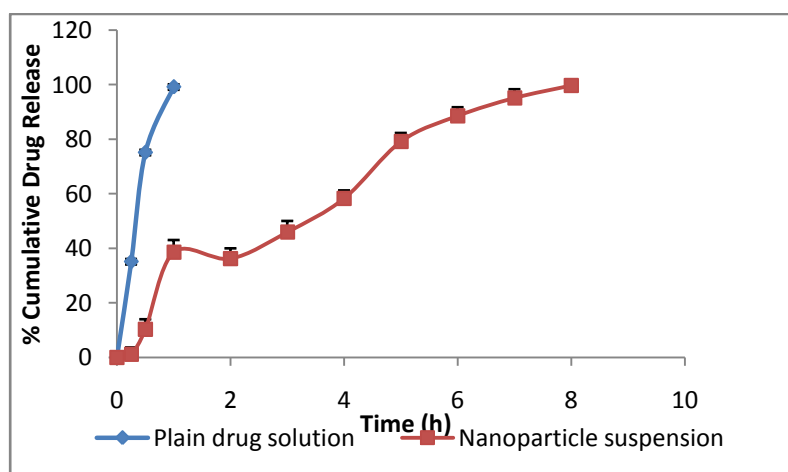


Figure 4.11: *In vitro* drug release profile for drug solution and nanoparticle suspension

4.7.4.7 *Ex vivo* drug diffusion studies

The drug release from plain drug solution was faster. Complete drug release was achieved in 2 hour. The nasal mucosa was a thicker barrier through which the drug molecules had to pass, and hence it became a rate limiting step. Therefore, the drug release from nanoparticles did not show a burst release in *ex vivo* diffusion. For the nanoparticles,  $98.12 \pm 3.18$  % drug was released in 8 h. The results can be seen in Table 4.15 and Figure 4.12.

Table 4.15: *Ex vivo* drug diffusion studies for plain drug solution and Galantamine hydrobromide loaded nanoparticles

| Time (hour) | Plain drug solution % Drug release $\pm$ SD | Nanoparticles % Drug release $\pm$ SD |
|-------------|---|---------------------------------------|
| 0           | 0   | 0                                     |
| 0.25        | $28.21 \pm 1.25$                            | $5.13 \pm 1.04$                       |
| 0.5         | $47.35 \pm 2.39$                            | $12.36 \pm 2.17$                      |
| 1           | $78.97 \pm 2.97$                            | $26.10 \pm 4.44$                      |
| 2           | $98.36 \pm 3.11$                            | $38.22 \pm 4.03$                      |
| 3           |   | $51.76 \pm 3.71$                      |
| 4           |   | $68.06 \pm 3.43$                      |
| 5           |   | $79.49 \pm 2.99$                      |
| 6           |   | $88.55 \pm 3.12$                      |
| 7           |   | $93.72 \pm 3.37$                      |
| 8           |   | $98.12 \pm 3.18$                      |

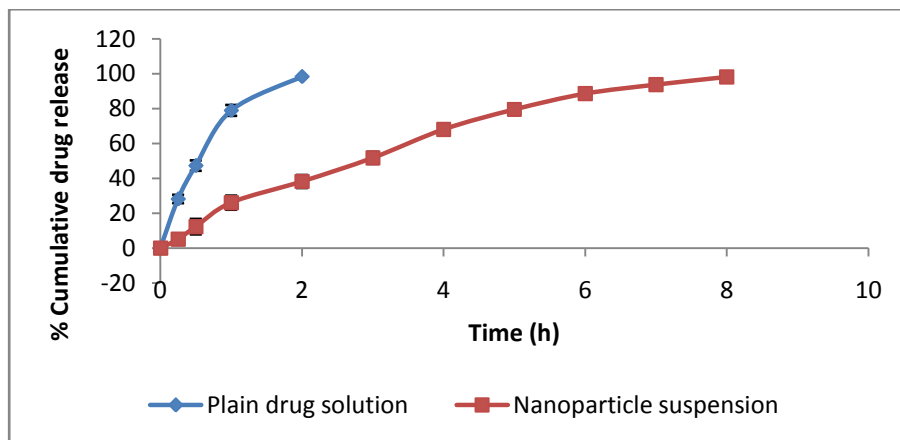


Figure 4.12: *Ex vivo* drug release profile for drug solution and nanoparticle suspension.

#### 4.8 Lyophilization of Galantamine hydrobromide loaded nanoparticles

Freeze drying causes increase in particle size of nanoparticles after lyophilization due to aggregation of particles during the process (Abdelwahed, Degobert, Stainmesse, & Fessi, 2006). If these aggregates are not separated during re-dispersion, it may cause instability to the system. The optimized Nanoparticle formulation was lyophilized using lyophilizer (Heto Drywinner, Vaccubrand, Denmark). Different cryoprotectants (Trehalose dehydrate, Mannitol and Sucrose) were used at different ratios to find out optimum concentration of cryoprotectant which showed minimum increment in particle size. The minimum increment of particle size was observed for 2% mannitol as cryoprotectant in the ratio of 1:1 w/w.

Table 4.16: Optimization of cryoprotectant for Galantamine hydrobromide loaded nanoparticles

| <b>Cryoprotectant</b>     | <b>Particle size after Lyophilization</b> | <b>Polydispersity Index</b> |
|---------------------------|---|-----------------------------|
| Trehalose dehydrate (1:1) | 267.12 ± 12.78                            | 0.31                        |
| Trehalose dehydrate (1:2) | 303.14 ± 14.55                            | 0.33                        |
| Trehalose dehydrate (1:3) | 289.47 ± 12.78                            | 0.24                        |
| Sucrose (1:1)             | 237.29 ± 18.96                            | 0.29                        |
| Sucrose (1:2)             | 278.31 ± 13.97                            | 0.33                        |
| Sucrose (1:3)             | 319.29 ± 15.39                            | 0.38                        |
| Mannitol (1:1)            | 138.27 ± 10.29                            | 0.37                        |
| Mannitol (1:2)            | 190.36 ± 14.39                            | 0.21                        |
| Mannitol (1:3)            | 200.94 ± 18.76                            | 0.20                        |

## 4.9 References

- Abdelwahed, W., Degobert, G., Stainmesse, S., & Fessi, H. (2006). Freeze-drying of nanoparticles: Formulation, process and storage considerations. *Advanced Drug Delivery Reviews*, 58(15), 1688-1713. doi: <https://doi.org/10.1016/j.addr.2006.09.017>
- AJ, M. (1984). Selection of subsets of regression variables. *J R Stat Soc Ser A*, 147, 389-425.
- Anhorn, M. G., Mahler, H. C., & Langer, K. (2008). Freeze drying of human serum albumin (HSA) nanoparticles with different excipients. *Int J Pharm*, 363(1-2), 162-169. doi: 10.1016/j.ijpharm.2008.07.004
- Elzoghby, A. O., Samy, W. M., & Elgindy, N. A. (2012). Albumin-based nanoparticles as potential controlled release drug delivery systems. *J Control Release*, 157(2), 168-182. doi: 10.1016/j.jconrel.2011.07.031
- FDA, U. (2012). Quality by Design for ANDAs: An Example for Immediate-Release Dosage Forms (Guideline). Retrieved 25th February, 2016 <http://www.fda.gov/downloads/Drugs/DevelopmentApprovalProcess/HowDrugsareDevelopedandApproved/ApprovalApplications/AbbreviatedNewDrugApplicationANDAGenerics/UCM304305.pdf>
- Fornaguera, C., Feiner-Gracia, N., Caldero, G., Garcia-Celma, M. J., & Solans, C. (2015). Galantamine-loaded PLGA nanoparticles, from nano-emulsion templating, as novel advanced drug delivery systems to treat neurodegenerative diseases. *Nanoscale*, 7(28), 12076-12084. doi: 10.1039/C5NR03474D
- Friese, A., Seiller, E., Quack, G., Lorenz, B., & Kreuter, J. (2000). Increase of the duration of the anticonvulsive activity of a novel NMDA receptor antagonist using poly(butylcyanoacrylate) nanoparticles as a parenteral controlled release system. *Eur J Pharm Biopharm*, 49(2), 103-109.
- Hanafy, A. S., Farid, R. M., & ElGamal, S. S. (2015). Complexation as an approach to entrap cationic drugs into cationic nanoparticles administered intranasally for Alzheimer's disease management: preparation and detection in rat brain. *Drug Dev Ind Pharm*, 41(12), 2055-2068. doi: 10.3109/03639045.2015.1062897
- ICH. (2009). Pharmaceutical Development (Q8). Retrieved 25/02/2016, from International Conference on Harmonisation [http://www.ich.org/fileadmin/Public\\_Web\\_Site/ICH\\_Products/Guidelines/Quality/Q8\\_R1/Step4/Q8\\_R2\\_Guideline.pdf](http://www.ich.org/fileadmin/Public_Web_Site/ICH_Products/Guidelines/Quality/Q8_R1/Step4/Q8_R2_Guideline.pdf)
- Johansson, J. S. (1997). Binding of the Volatile Anesthetic Chloroform to Albumin Demonstrated Using Tryptophan Fluorescence Quenching. *Journal of Biological Chemistry*, 272(29), 17961-17965. doi: 10.1074/jbc.272.29.17961
- Kan, S., Lu, J., Liu, J., Wang, J., & Zhao, Y. (2014). A quality by design (QbD) case study on enteric-coated pellets: Screening of critical variables and establishment of design space at laboratory scale. *Asian Journal of Pharmaceutical Sciences*, 9(5), 268-278. doi: <http://dx.doi.org/10.1016/j.ajps.2014.07.005>

- Levison, K. K., Takayama, K., Isowa, K., Okabe, K., & Nagai, T. (1994). Formulation optimization of indomethacin gels containing a combination of three kinds of cyclic monoterpenes as percutaneous penetration enhancers. *J Pharm Sci*, 83(9), 1367-1372.
- Mak, K. W. Y., Yap, M. G. S., & Teo, W. K. (1995). Formulation and optimization of two culture media for the production of tumour necrosis factor- $\beta$  in *Escherichia coli*. *Journal of Chemical Technology & Biotechnology*, 62(3), 289-294. doi: 10.1002/jctb.280620312
- Matharu, B., Gibson, G., Parsons, R., Huckerby, T. N., Moore, S. A., Cooper, L. J., . . . Austen, B. (2009). Galantamine inhibits beta-amyloid aggregation and cytotoxicity. *J Neurol Sci*, 280(1-2), 49-58. doi: 10.1016/j.jns.2009.01.024
- Merodio, M., Arnedo, A., Renedo, M. J., & Irache, J. M. (2001). Ganciclovir-loaded albumin nanoparticles: characterization and in vitro release properties. *Eur J Pharm Sci*, 12(3), 251-259.
- Mitra, S., Gaur, U., Ghosh, P. C., & Maitra, A. N. (2001). Tumour targeted delivery of encapsulated dextran-doxorubicin conjugate using chitosan nanoparticles as carrier. *J Control Release*, 74(1-3), 317-323.
- Moribe, K., Limwikrant, W., Higashi, K., & Yamamoto, K. (2012). Structural evaluation of probucol nanoparticles in water by atomic force microscopy. *Int J Pharm*, 427(2), 365-371. doi: 10.1016/j.ijpharm.2012.02.020
- Mufamadi, M. S., Choonara, Y. E., Kumar, P., Modi, G., Naidoo, D., van Vuuren, S., . . . Pillay, V. (2013). Ligand-functionalized nanoliposomes for targeted delivery of galantamine. *Int J Pharm*, 448(1), 267-281. doi: 10.1016/j.ijpharm.2013.03.037
- Pallagi, E., Ambrus, R., Szabo-Revesz, P., & Csoka, I. (2015). Adaptation of the quality by design concept in early pharmaceutical development of an intranasal nanosized formulation. *Int J Pharm*, 491(1-2), 384-392. doi: 10.1016/j.ijpharm.2015.06.018
- Patel, Y., Poddar, A., Sawant, K., & (2014). Improved Oral Bioavailability of Cefuroxime Axetil Utilizing Nanosuspensions Developed by Media Milling Technique. *Pharmaceutical Nanotechnology*, 2(2), 75-86. doi: 10.2174/2211738502666140804233343
- Peracchia, M. T., Fattal, E., Desmaele, D., Besnard, M., Noel, J. P., Gomis, J. M., . . . Couvreur, P. (1999). Stealth PEGylated polycyanoacrylate nanoparticles for intravenous administration and splenic targeting. *J Control Release*, 60(1), 121-128.
- Qi, L., Guo, Y., Luan, J., Zhang, D., Zhao, Z., & Luan, Y. (2014). Folate-modified bexarotene-loaded bovine serum albumin nanoparticles as a promising tumor-targeting delivery system. *Journal of Materials Chemistry B*, 2(47), 8361-8371. doi: 10.1039/C4TB01102C
- Rahman, Z., Zidan, A. S., Habib, M. J., & Khan, M. A. (2010). Understanding the quality of protein loaded PLGA nanoparticles variability by Plackett-Burman design. *Int J Pharm*, 389(1-2), 186-194. doi: 10.1016/j.ijpharm.2009.12.040
- Seju, U., Kumar, A., & Sawant, K. K. (2011). Development and evaluation of olanzapine-loaded PLGA nanoparticles for nose-to-brain delivery: In vitro and

- in vivo studies. *Acta Biomaterialia*, 7(12), 4169-4176. doi: <http://dx.doi.org/10.1016/j.actbio.2011.07.025>
- Shah, B., Khunt, D., Bhatt, H., Misra, M., & Padh, H. (2015). Application of quality by design approach for intranasal delivery of rivastigmine loaded solid lipid nanoparticles: Effect on formulation and characterization parameters. *Eur J Pharm Sci*, 78, 54-66. doi: 10.1016/j.ejps.2015.07.002
  - Shirakura O, Yamada M, Hahimoto M, Ishimaru S, Takayama K, & Nagai, T. (1991). Particle - size Design Using Computer Optimization Technique. *Drug Dev Ind Pharm*, 17, 471-483.
  - Tantra, R., Tompkins, J., & Quincey, P. (2010). Characterisation of the de-agglomeration effects of bovine serum albumin on nanoparticles in aqueous suspension. *Colloids Surf B Biointerfaces*, 75(1), 275-281. doi: 10.1016/j.colsurfb.2009.08.049
  - V De Caro, G Giandalia, MG Siragua, G Campsisi, & Giannola, L. (2009). Galantamine delivery on Buccal mucosa: Permeation enhancement and design of matrix tablets. *J Bioequiv Availab*(1), 127-134. doi: 10.4172/jbb.1000020
  - Verma, S., Lan, Y., Gokhale, R., & Burgess, D. J. (2009). Quality by design approach to understand the process of nanosuspension preparation. *Int J Pharm*, 377(1-2), 185-198. doi: 10.1016/j.ijpharm.2009.05.006
  - Vogt, F. G., & Kord, A. S. (2011). Development of quality-by-design analytical methods. *J Pharm Sci*, 100(3), 797-812. doi: 10.1002/jps.22325
  - Wagner, J. M., & Shimshak, D. G. (2007). Stepwise selection of variables in data envelopment analysis: Procedures and managerial perspectives. *European Journal of Operational Research*, 180(1), 57-67. doi: <http://dx.doi.org/10.1016/j.ejor.2006.02.048>
  - Wagner, S., Rothweiler, F., Anhorn, M. G., Sauer, D., Riemann, I., Weiss, E. C., . . . Langer, K. (2010). Enhanced drug targeting by attachment of an anti alphav integrin antibody to doxorubicin loaded human serum albumin nanoparticles. *Biomaterials*, 31(8), 2388-2398. doi: 10.1016/j.biomaterials.2009.11.093
  - Wilson, B., Samanta, M. K., Santhi, K., Kumar, K. P., Ramasamy, M., & Suresh, B. (2010). Chitosan nanoparticles as a new delivery system for the anti-Alzheimer drug tacrine. *Nanomedicine*, 6(1), 144-152. doi: 10.1016/j.nano.2009.04.001
  - Yerlikaya, F., Ozgen, A., Vural, I., Guven, O., Karaagaoglu, E., Khan, M. A., & Capan, Y. (2013). Development and evaluation of paclitaxel nanoparticles using a quality-by-design approach. *J Pharm Sci*, 102(10), 3748-3761. doi: 10.1002/jps.23686
  - Yu, L. X. (2008). Pharmaceutical quality by design: product and process development, understanding, and control. *Pharm Res*, 25(4), 781-791. doi: 10.1007/s11095-007-9511-1